High order sliding mode control of a DFIM supplied by two power inverters

[*]Zinelaabidine Boudjema, Rachid Taleb
Laboratoire Génie Electrique et Energies Renouvelables (LGEER), Electrical Engineering Department
Hassiba Benbouali University, Chlef, Algeria.
[*]Boudjemaa1983@yahoo.fr

[**]Adil Yahdou, Housseyn Kahal
Electrical Engineering Department
Hassiba Benbouali University, Chlef, Algeria
[**]yahdou10h@yahoo.fr

***Abstract*—Traditional vector control structures which include proportional-integral (PI) regulator for the speed of a doubly fed induction motor (DFIM) driven have some disadvantages such as parameter tuning complications, mediocre dynamic performances and reduced robustness. Thus, based on the analysis of the mathematical model of a DFIM supplied by two indirect inverters, this paper addresses a non-linear control algorithm based on high order sliding mode. The conventional sliding mode control has large chattering on the electromagnetic torque developed by the DFIM. In order to solve this problem, the second order sliding mode technique is used. The simulation results show the effectiveness of the proposed method especially in chattering-free behavior, response to sudden load torque variations and robustness against machine parameters variations.**

Keywords—doubly fed induction motor (DFIM); power inverter; speed control; second order sliding mode.

I. INTRODUCTION

The doubly fed induction motor (DFIM) is a very interesting solution for variables speed applications such as wind energy conversion systems and electric vehicles [1,2]. Therefore, it covers all power ranges. Obviously, the requested variable speed domain and the desired performances depend on the application types [3].

The DFIM has several different advantages compared to the usual squirrel-cage machine. The DFIM can be controlled from the stator or rotor by different possible combinations [4].

In [5], a study on a DFIM with constant stator frequency and vector control is described. DFIM stator is directly supplied by the grid, and a cyclo-converter feeds the rotor windings. The main drawback of this configuration is the speed operating range limited to 20%-25% of the nominal speed.

A novel high-power inverter drive system is exposed in [6,7]. Principles and experimental investigations are presented and discussed. The authors used a DFIM configuration that is supplied by pulse width modulation (PWM) inverters that are linked with current controllers. In this configuration, each side of the machine is fed by a dc-link ac/ac inverter. The stator and the rotor windings do not have the same voltage rating; a step-down transformer between the ac network and the three-phase rectifier of the rotor winding supply is added. This drive can be used in industrial applications, such as steel rolling mill or marine propulsion systems.

A lot of works have been presented with diverse control diagrams of DFIM. These control diagrams are usually based on vector control notion with conventional PI controllers.

Recently, the sliding mode control (SMC) method has been widely used for robust control of nonlinear systems. Several papers have been published based on (SMC) of DFIG [8,9].

The SMC achieves robust control by adding a discontinuous control signal across the sliding surface, satisfying the sliding condition. Nevertheless, this type of control has an essential disadvantage, which is the chattering phenomenon caused by the discontinuous control action. To treat these difficulties, several modifications to the original sliding control law have been proposed, the most popular being the boundary layer approach [10, 11].

The paper is structured as follows: the doubly fed induction machine (DFIM) model and the vector control strategy are respectively discussed in sections 2 and 3. Session 4 shows the synthesis of the different controllers applied on the speed control of the DFIM. The effectiveness of the proposed controller (SOSMC) verified by simulation is presented in section 5. Finally, the main conclusions of the work are drawn.

II. THE DFIM MODEL

Its dynamic model expressed in the synchronous reference frame is given by :

$$\begin{aligned} \bar{V}_S &= R_S \bar{I}_S + \frac{d\bar{\varphi}_S}{dt} + j\omega_S \bar{\varphi}_S \\ \bar{V}_R &= R_R \bar{I}_R + \frac{d\bar{\varphi}_R}{dt} + j\omega_R \bar{\varphi}_R \end{aligned} \quad (1)$$

$$\begin{aligned} \bar{\varphi}_S &= L_S \bar{I}_S + M_{SR} \bar{I}_R \\ \bar{\varphi}_R &= L_R \bar{I}_R + M_{SR} \bar{I}_S \end{aligned} \quad (2)$$

From (1) and (2), the state-all-current model is written as :

$$\begin{aligned}\frac{d\bar{I}_S}{dt} &= -\frac{R_S}{\sigma L_S}\bar{I}_S + \frac{M_{SR}R_R}{\sigma L_S L_R}\bar{I}_R + \frac{1}{\sigma L_S}\bar{V}_S - \frac{M_{SR}}{\sigma L_S L_R}\bar{V}_R \\ \frac{d\bar{I}_R}{dt} &= -\frac{R_R}{\sigma L_R}\bar{I}_R + \frac{M_{SR}R_S}{\sigma L_S L_R}\bar{I}_S + \frac{1}{\sigma L_R}\bar{V}_R - \frac{M_{SR}}{\sigma L_S L_R}\bar{V}_S\end{aligned} \quad (3)$$

This electrical model is completed by mechanical equation :

$$C_{em} - \frac{f\omega}{p} - C_r = \frac{J}{p}\frac{d\omega}{dt} \quad (4)$$

With :

$$\begin{cases}\omega = p\Omega \\ C_{em} = pM_{SR}.\mathrm{Im}(\bar{I}_S\bar{I}_S^{*})\end{cases} \quad (5)$$

III. Control strategy of the DFIM

A. Rotor flux orientation

In this section, the DFIM model can be described by the following state equations whose axis *d* is aligned with the rotor flux vector (see figure 1) [12] :

$$\varphi_{Rq} = 0 \;\; ; \;\; \varphi_R = \varphi_{Rd} \quad (6)$$

So, using equation (2) we can write :

$$I_{Rq} = -\frac{M_{SR}}{L_R}.I_{Sq} \quad (7)$$

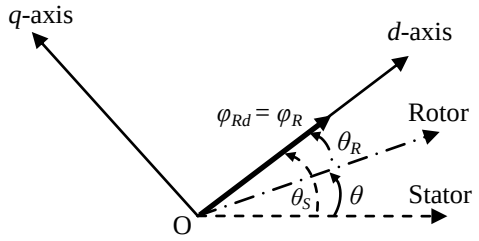

Fig. 1. Rotor field orientation on the *d*-axis.

Two methods can be used for motor magnetization [12] :

- Work with a unit power-factor in the stator or the rotor, which implies that one of the two currents, I_{Sd} or I_{Rd}, will be equal to zero,
- Divide the magnetizing current to equality between the two converters as follows :

$$I_{Sd} = I_{Rd} = \frac{I_d}{2}, \;\; \text{soit :}\; \varphi_{Rd} = (L_R + M_{SR})\frac{I_d}{2} \quad (8)$$

Choose I_{Rd} = 0 give the same expression to the stator and air-gap flux [12]. Moreover, the flux expression depends only on M_{SR} and the rotor power-factor will be equal the unit.

B. The current loops design

In order to obtain a decoupling between *d* and *q* axis, let us define new voltages as [12] :

$$\begin{cases}V_{tSq} = V_{Sq} - \frac{M_{SR}}{L_R}V_{Rq} \\ V_{tRq} = V_{Rq} - \frac{M_{SR}}{L_S}V_{Sq}\end{cases}, \begin{cases}V_{tSd} = V_{Sd} - \frac{M_{SR}}{L_R}V_{Rd} \\ V_{tRd} = V_{Rd} - \frac{M_{SR}}{L_S}V_{Sd}\end{cases} \quad (9)$$

Using equations (2), (6) and (9), we can write :

$$\begin{cases}V_{tSd} = R_S I_{Sd} + \sigma L_S \frac{dI_{Sd}}{dt} - R_R \frac{M_{SR}}{L_R} I_{Rd} - \varphi_{Sq}\omega_S + \frac{M_{SR}}{L_R}\varphi_{Rq}\omega_R \\ V_{tSq} = R_S I_{Sq} + \sigma L_S \frac{dI_{Sq}}{dt} - R_R \frac{M_{SR}}{L_R} I_{Rq} + \varphi_{Sd}\omega_S - \frac{M_{SR}}{L_R}\varphi_{Rd}\omega_R \\ V_{tRd} = R_R I_{Rd} + \sigma L_R \frac{dI_{Rd}}{dt} - R_S \frac{M_{SR}}{L_S} I_{Sd} - \varphi_{Rq}\omega_R + \frac{M_{SR}}{L_S}\varphi_{Sq}\omega_S \\ V_{tRq} = R_R I_{Rq} + \sigma L_R \frac{dI_{Rq}}{dt} - R_S \frac{M_{SR}}{L_S} I_{Sq} + \varphi_{Rd}\omega_R - \frac{M_{SR}}{L_S}\varphi_{Sd}\omega_S\end{cases} \quad (10)$$

Thus:

$$\begin{cases}V_{tSd} = V_{tSdc} + V_{tSdc1} = R_S I_{Sd} + \sigma L_S \frac{dI_{Sd}}{dt} + V_{tSdc1} \\ V_{tSq} = V_{tSqc} + V_{tSqc1} = R_S I_{Sq} + \sigma L_S \frac{dI_{Sq}}{dt} + V_{tSqc1} \\ V_{tRd} = V_{tRdc} + V_{tRdc1} = R_R I_{Rd} + \sigma L_R \frac{dI_{Rd}}{dt} + V_{tRdc1} \\ V_{tRq} = V_{tRqc} + V_{tRqc1} = R_R I_{Rq} + \sigma L_R \frac{dI_{Rq}}{dt} + V_{tRqc1}\end{cases} \quad (11)$$

This method gives the same transfer function between the currents and voltages of the same axis as shown by the following equation :

$$\begin{cases}\frac{I_{Sq}(s)}{V_{tSqc}(s)} = \frac{I_{Sd}(s)}{V_{tSd}(s)} = \frac{1}{R_S + \sigma L_S . s} \\ \frac{I_{Rq}(s)}{V_{trqc}(s)} = \frac{I_{Rd}(s)}{V_{tRd}(s)} = \frac{1}{R_R + \sigma L_R . s}\end{cases} \quad (12)$$

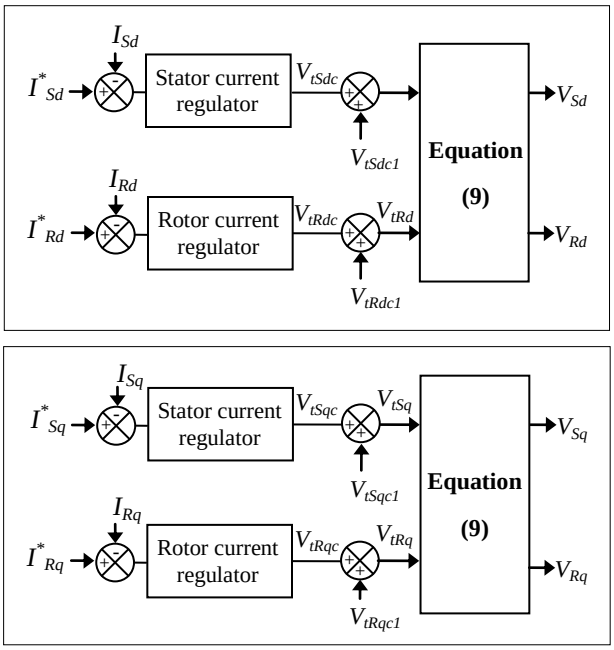

Fig. 2. Decoupling and regulation of the currents.

The current references are given by :

$$\begin{cases} I_{Sd}^{\ *} = \dfrac{1}{M_{SR}}\varphi_{Rd}^{\ *}, \quad I_{Sq}^{\ *} = \dfrac{L_R}{p.M_{SR}.\varphi_{Rd}^{\ *}}\ C_{em}^{\ *} \\ I_{Rd}^{\ *} = 0 \qquad\quad , \quad I_{Rq}^{\ *} = -\dfrac{1}{p.\varphi_{Rd}^{\ *}}\ C_{em}^{\ *} \end{cases} \tag{13}$$

Thus, figure 2 shows the control structure of the currents.

C. The speed regulation

Basing on relation (6) and the assumption to work with I_{Rd} equal to zero, the electromagnetic torque can be written as :

$$C_{em} = -p\,\varphi_{Rd} I_{Rq} = K_{em} I_{Rq} \tag{14}$$

Substituting (24) in (13), it results :

$$J\frac{d\Omega}{dt} = K_{em} I_{Rq} - f\,\Omega - C_r \tag{15}$$

Where K_{em} is the torque constant.

Thus, the speed transfer function can be expressed by:

$$\Omega(s) = \frac{K_{em}}{f + Js} I_{Rq}(s) - \frac{1}{f + Js} C_r(s) \tag{16}$$

$C_r(s)$ is a disturbing input, while $I_{Sq}(s)$ is main input.

Consequently, the block diagram of the speed regulation is given by figure 3.

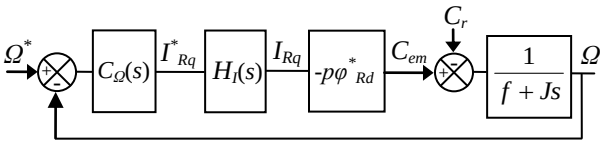

Fig. 3. Block diagram of the speed control.

IV. Speed controllers synthesis

In this section, we have chosen to compare the performances of the DFIM with three different controllers: Proportional integral (PI), conventional sliding mode (SMC), and second order sliding mode (SOSMC).

A. Sliding mode controller (SMC)

The sliding mode technique is developed from variable structure control to solve the disadvantages of other designs of nonlinear control systems. The sliding mode is a technique to adjust feedback by previously defining a surface. The system which is controlled will be forced to that surface, then the behavior of the system slides to the desired equilibrium point [13].

The main feature of this control is that we only need to drive the error to a *switching surface*. When the system is in *sliding mode*, the system behavior is not affected by any modeling uncertainties and/or disturbances. The design of the control system will be demonstrated for a nonlinear system presented in the canonical form [14,15] :

$$\dot{x} = f(x,t) + B(x,t)V(x,t),\ x \in R^n,\ V \in R^m, ran(B(x,t)) = m \tag{17}$$

with control in the sliding mode, the goal is to keep the system motion on the manifold S, which is defined as :

$$S = \{x : e(x, t) = 0\} \tag{18}$$

$$e = x^* - x \tag{19}$$

Here e is the tracking error vector, $\boldsymbol{x}^*$ is the desired state, x is the state vector. The control input u has to guarantee that the motion of the system described in (17) is restricted to belong to the manifold S in the state space. The sliding mode control should be chosen such that the candidate Lyapunov function satisfies the Lyapunov stability criteria :

$$\vartheta = \frac{1}{2} S(x)^2, \tag{20}$$

$$\dot{\vartheta} = S(x)\dot{S}(x). \tag{21}$$

This can be assured for :

$$\dot{\vartheta} = -\eta |S(x)| \tag{22}$$

Here η is strictly positive.
Essentially, equation (20) states that the squared "distance" to the surface, measured by $e(x)^2$, decreases along all system trajectories. Therefore (21), (22) satisfy the Lyapunov condition. With selected Lyapunov function the stability of the whole control system is guaranteed. The control function will satisfy reaching conditions in the following form:

$$U^{com} = U^{eq} + U^{n} \tag{23}$$

Here U^{com} is the control vector, U^{eq} is the equivalent control vector, U^{n} is the correction factor and must be calculated so that the stability conditions for the selected control are satisfied.

$$U^{n} = K\ \mathrm{sat}((\mathrm{S(x)}/\delta) \tag{24}$$

sat(($S(x)/\delta$) is the proposed saturation function, δ is the boundary layer thickness. In this paper we propose the Slotine method [16]:

$$S(X) = \left(\frac{d}{dt} + \lambda\right)^{n-1} e \tag{25}$$

Here, e is the tracking error vector, λ is a positive coefficient and n is the relative degree.

In our study, we choose the error between the measured and reference speed of the DFIM as sliding mode surface, so we can write the following expression :

$$S = \Omega^{*} - \Omega \tag{26}$$

The first order derivate of (26), gives :

$$\dot{S} = \dot{\Omega}^{*} - \dot{\Omega} \tag{27}$$

Substituting the expression of $\dot{\Omega}$ equation (16) in equation (27), we obtain:

$$\dot{S} = \dot{\Omega}^{*} - \frac{K_{em}}{J} I_{Rq} - \frac{f}{J}\ \Omega - \frac{C_r}{J} \tag{28}$$

I_{qr} will be the component of the control vector used to constraint the system to converge to $S = 0$. The control vector U_{eq} is obtain by imposing $\dot{S} = 0$ so the equivalent control components are given by the following relation :

$$U_{eq} = -\frac{f}{K_{em}} \cdot \Omega + \frac{J}{K_{em}} \dot{\Omega}^{*} - \frac{C_r}{K_{em}} \tag{29}$$

To obtain good performances, dynamic and commutation around the surface, the control vector is imposed as follows [14]:

$$U = U_{eq} + K \cdot \mathrm{sign}(S) \tag{30}$$

The sliding mode will exist only if the following condition is met:

$$S \cdot \dot{S} < 0 \tag{31}$$

B. Second order sliding mode controller (SOSMC)

Sliding mode control (SMC) is one of the most interesting nonlinear control approaches. Nevertheless, a few drawbacks arise in its practical implementation, such as chattering phenomenon and undesirable mechanical effort [17]. In order to reduce the effects of these problems, second order sliding mode seems to be a very attractive solution [18].

This method generalizes the essential sliding mode idea by acting on the higher order time derivatives of the sliding manifold, instead of influencing the first time derivative as it is the case in SMC, therefore reducing chattering and avoiding strong mechanical efforts while preserving SMC advantages [19].

In order to ensure the DFIM's speed convergence to their reference, a second order sliding mode control (SOSMC) is used. Considering the sliding mode surface given by (29), the following expression can be written:

$$\begin{cases} \dot{S} = \dot{\Omega}^{*} - \dfrac{K_{em}}{J} I_{Rq} - \dfrac{f}{J}\ \Omega - \dfrac{C_r}{J} \\ \ddot{S} = Y(t,x) + \Lambda(t,x) I_{Rq} \end{cases} \tag{42}$$

Where $Y(t,x)$ and $\Lambda(t,x)$ are uncertain functions which satisfy:

$$Y > 0,\ |Y| > \lambda,\ 0 < K_m < \Lambda < K_M$$

Basing on the super twisting algorithm introduced by Levant in [19], the proposed high order sliding mode controller contains two parts :

$$I_{Rq} = v_1 + v_2 \tag{43}$$

With

$$\dot{v}_1 = -k \cdot sign(S)$$
$$v_2 = -l \cdot |S|^{\gamma} \cdot sign(S)$$

In order to ensure the convergence of the sliding manifolds to zero in finite time, the gains can be chosen as follows [20].

$$\begin{cases} k > \dfrac{\lambda}{K_m} \\ l^2 \geq \dfrac{4\lambda}{K_m^2} \dfrac{K_M (k+\lambda)}{K_m (k-\lambda)} \\ 0 < \gamma \leq 0.5 \end{cases}$$

V. Simulation Results and Discussions

In this section, simulations are realized with a 1.5 KW motor coupled to a 220V/50Hz grid. The bloc diagram of the proposed control scheme of the DFIM is given by figure 4. Parameters of the machine are given in appendix. In the aim to evaluate the performances of the four controllers: PI, SMC and SOSMC, three categories of tests have been realized: pursuit test, sensitivity to the load torque variation and robustness against machine parameter variations.

A. *Pursuit test*

The objective of this test is the study of the three controllers' behavior in reference tracking, while the load torque is considered equal to zero. The simulation results are presented in figures 5 and 6. As it's shown by figure 5, for the three controllers, the mechanical speed tracks almost perfectly their reference but with an important response time for the PI controller compared to the other controllers. Therefore it can be considered that the two types of sliding mode controllers have a very good performance for this test. On the other hand, figure 6 shows the harmonic spectrum of the electromagnetic torque of the DFIM obtained using Fast Fourier Transform (FFT) technique for the two types of sliding mode controllers. It can be observed that the total harmonic distortion (THD) is clearly reduced for SOSMC (THD = 45.78%) when compared to SMC (THD = 49.62%). Therefore it can be concluded that the proposed controller (SOSMC) is effective in eliminating chattering phenomenon. However, we note that despite the use of SOSMC, THD torque remains fairly high. This is principally due to the use of two power converters, which represents one of the major disadvantages of such configuration of DFIM.

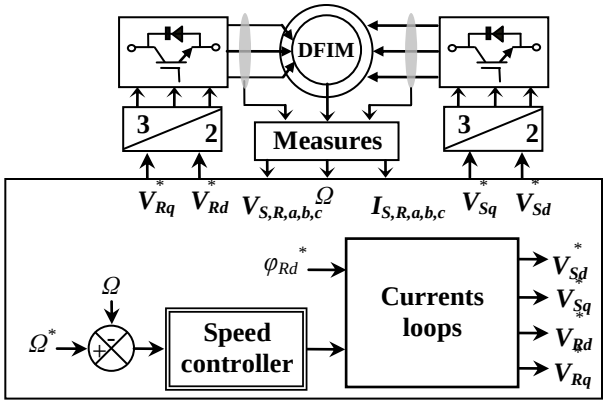

Fig. 4. Block diagram of the proposed control scheme of the DFIM.

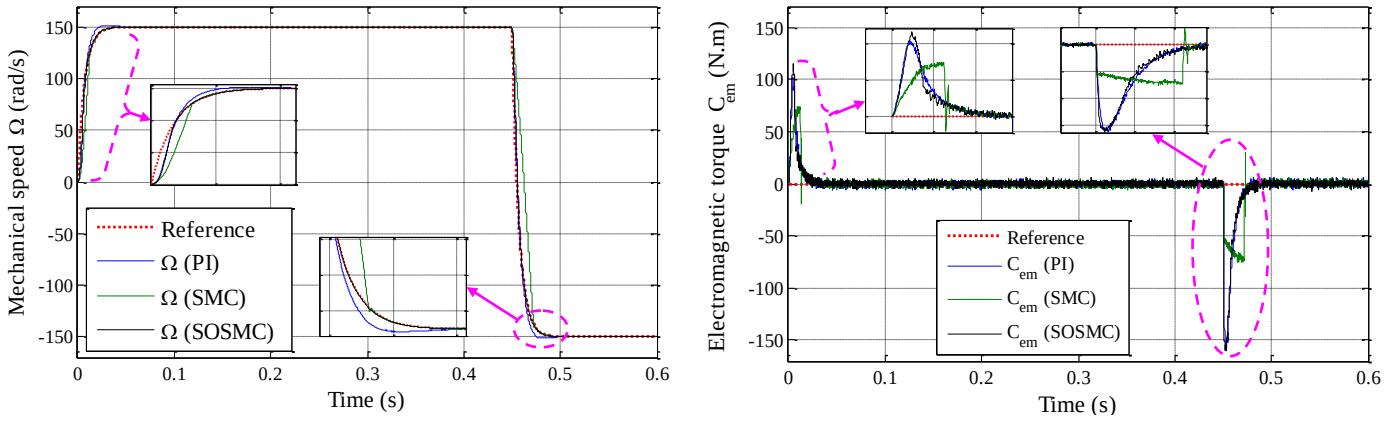

Fig. 5. Reference tracking test.

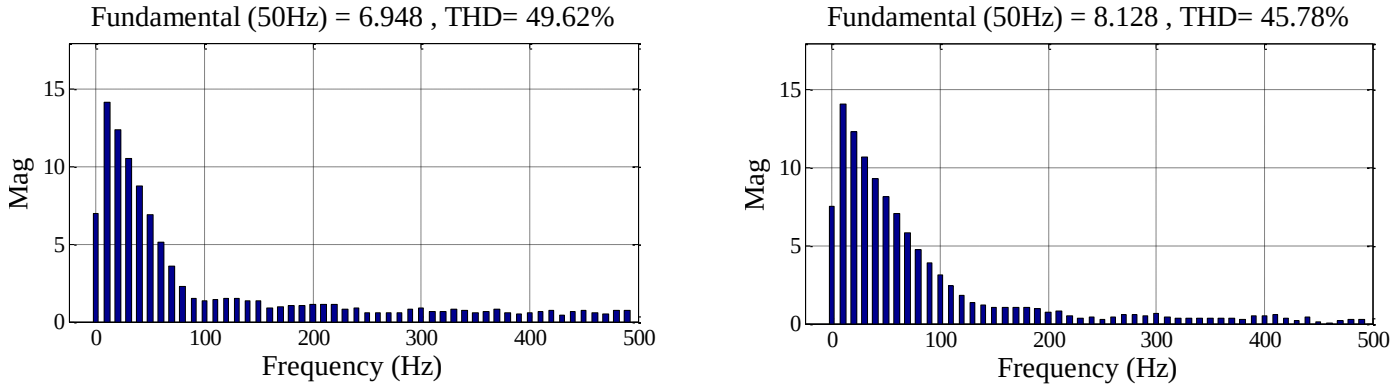

Fig. 6. Spectrum harmonic of the electromagnetic torque for (a) SMC, (b) SOSMC.

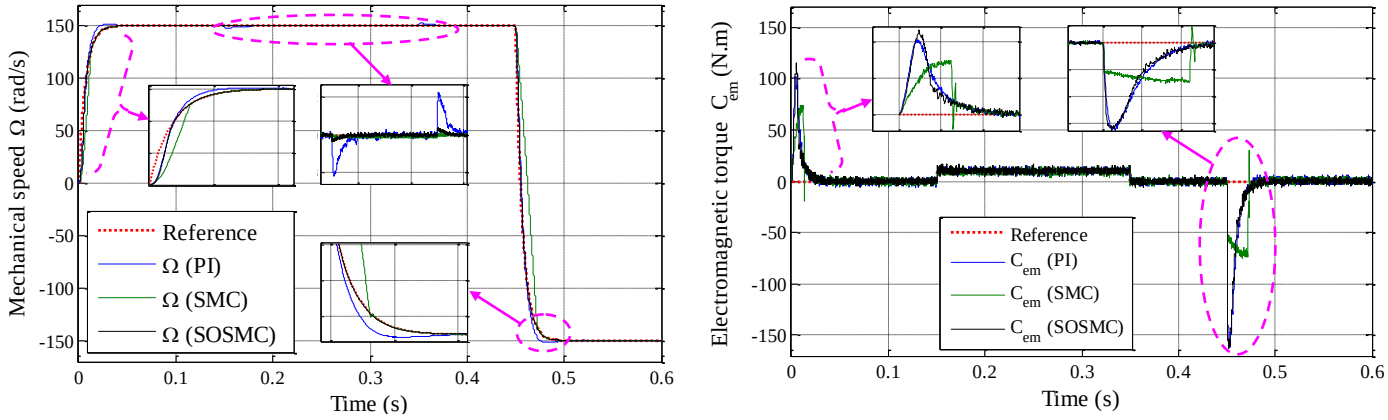

Fig. 7. Sensitivity to the load torque variation.

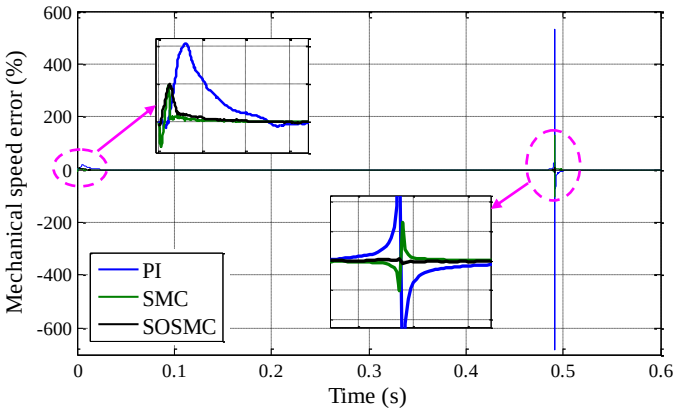

Fig. 8. Robustness test (J=2*J_n).

B. *Sensitivity to the load torque variation*

The aim of this test is to analyze the influence of the load torque variation on the DFIM response for the three controllers. For this objective and in the in the time interval t = 0.15s and t = 0.35s, the load torque is kept equal to its nominal value C_{rn} =10 N.m. The simulation results are shown in figure 7. This figure express that the effect produced by the load torque variation is very clear on the speed curve of the system with PI controller, while the effects are almost negligible for the system with the two other controllers. It can be noticed that these last have a nearly perfect speed disturbance rejection, indeed; only very small speed variations can be observed (fewer than 2%). This result is very attractive for speed control applications to ensure stability when the load torque is varying.

C. *Robustness*

In order to test the robustness of the used controllers, the machine inertia has been doubled. The results presented in figure 8 show that inertia variation presents a clear effect on the speed responses (in the error curves) of all used controllers and that the effect appears more significant for PI controller than that with the two other ones. Thus it can be concluded that these last are robust against this parameter variation.

VI. Conclusion

A new robust control method based on variable structure technique of a doubly fed induction motor supplied by two power inverters has been presented in this paper. In the first step, we started with a study of modeling on the DFIM. In second step, we adopted a vector control strategy in order to make the behavior of the DFIM like a DC motor, i.e. a decoupling between the magnetic flux and the electromagnetic torque. Three types of controllers are synthesized and compared in the third step in the goal to control the speed of the DFIM. The various results obtained in simulation show the SOSMC robustness to the system and load parameters disturbances. In addition the speed follow without overshooting, decoupling, stability and equilibrium convergence are ensured on the entire variation interval. The results obtained with this SOSMC are very interesting compared to the conventional sliding mode controller especially in eliminating of the chattering phenomenon. The

static inverter and the control nature with variable structure introduce high frequency undulations which appear on the torque level. However, with the use of second order sliding mode and a high modulation index, we can reduce the couple fluctuations considerably. Moreover this control has the advantage of being easily implemented by a program control.

APPENDIX

TABLE I. NOMENCLATURE.

Symbol	Significance
S, R	Rotor and stator indices,
d, q	Direct and quadrate indices for orthogonal components,
$\bar{X}$	Variable complex such as: $\bar{x} = \mathrm{Re}[\bar{x}] + j\ \mathrm{Im}[\bar{x}]$ with $j^2 = -1$. $\bar{X}$ it can be a voltage as $\bar{V}$, a current as $\bar{I}$ or a field as $\bar{\varphi}$,
R_S, R_R	Stator and rotor resistances,
L_S, L_R	Stator and rotor inductances,
M_{SR}	Mutual inductance,
p	Number of pairs poles,
θ	Absolute rotor position,
θ_S, θ_R	Stator and rotor flux absolute positions,
σ	Leakage flux total coefficient $(\sigma = 1 - M_{SR}^{\ 2} / L_S L_R)$,
ω_S	Stator current frequency (rad/s),
J	Inertia (J_n nominal value of J),
f	Coefficient of viscous frictions,
C_r	Load torque,
C_{em}	Electromagnetic torque.

TABLE II. THE DFIM PARAMETERS.

Parameters	Value	IS-Unit
Stator voltage	220	V
Rotor voltage	130	V
Stator/rotor frequency	50	Hz
Stator resistance	1.75	Ω
Rotor resistance	1.68	Ω
Stator inductance	0.295	H
Rotor inductance	0.104	H
Mutual inductance	0.165	H
Inertia	0.01	$Kg.m^2$

REFERENCES

[1] O. Anaya-Lara, N. Jenkins, N., Ekanayake, J., Cartwright, P., Hughes, M.: *Wind energy generation*. In: Wiley, 2009.

[2] Y. Djeriri, A. Meroufel, A. Massoum and Z. Boudjema, "A comparative study between field oriented control strategy and direct power control strategy for DFIG," In: Journal of Electrical Engineering, Vol. 14, No. 2, pp. 159-167, 2014.

[3] M. A. Pöller, "Doubly-fed induction machine models for stability assessment of wind farms," In: Proc. IEEE PowerTech, Bologna, Italy, Vol. 3, 23-26 June 2003.

[4] T. Brekken and N. Mohan, "A novel doubly-fed induction wind generator control scheme for reactive power control and torque pulsation compensation under unbalanced grid voltage conditions," In: IEEE 34th Annual Power Electronics Specialist Conference, 2003, PESC'03, Vol. 2, pp. 760-764, 15-19 June 2003.

[5] W. Leonhard, "Control of electrical drives," In: 2nd ed. New York: Springer-Verlag, 1996.

[6] Y. Kawabata, E. Ejiogu and T. Kawabata, "Vector controlled double inverter fed wound rotor induction motor suitable for high power drives," In: IEEE Trans. Ind. Appl., Vol. 35, No. 5, pp. 1058-1066, Sep./Oct. 1999.

[7] F. Bonnet, P. E. Vidal and M. Pietrzak-David, "Dual direct torque control of doubly fed induction machine," In: IEEE Trans On Industrial Electronics, Vol. 54, No. 5, October 2007.

[8] M. I. Martinez, G. Tapia, A. Susperregui and H. Camblong, "Sliding-mode control for DFIG rotor and grid-side converters under unbalanced and harmonically distorted grid voltage," In: IEEE Trans. On Energy Conversion, Vol. 27, No. 2, pp. 328-339, March 2000.

[9] J. Hu, H. Nian, B. Hu, Y. He and Z. Q. Zhu, "Direct active and reactive power regulation of DFIG using sliding-mode control approach," In: IEEE Trans. On Energy Conversion, Vol. 25, No. 4, pp. 1028–1039, Dec. 2010.

[10] J. Lopez, P. Sanchis, X. Roboam and L. Marroyo, "Dynamic behavior of the doubly fed induction generator during three-phase voltage dips," In: IEEE Trans. on Energy Conversion, pp.709-717, 22 (Sept.(3)) 2007.

[11] F. Cupertino, D. Naso, E. Mininno, B. Turchiano, "Sliding-mode control with double boundary layer for robust compensation of payload mass and friction in linear motors," In: IEEE Trans. On Trans. Ind. Appl., Vol. 45, No. 5, pp. 1688-1696, Sep./Oct 2009.

[12] K. E. Okedu, R. Uhunmwangho, "Matrix converter control for DFIG," In Proc. of IEEE International Conference on Emerging & Sustainable Technologies for Power & ICT in a Developing Society (NIGERCON), pp. 273-277, 14-16 November 2013.

[13] R. J. Wai and J. M. Chang, "Implementation of robust wavelet-neural-network sliding-mode control for induction servo motor drive," In: IEEE Trans. On Ind. Elec, Vol. 50, No. 6, pp.1317-1334, December 2003.

[14] T. Sun, Z. Chen and F. Blaabjerg, "Flicker study on variable speed wind turbines with doubly fed induction generators," In: IEEE Transactions on Energy Conversion, pp. 896–905, 20 (December (4)) 2005.

[15] Z. Boudjema, A. Meroufel and Y. Djerriri, "Nonlinear control of a doubly fed induction generator for wind energy conversion," In: Carpathian Journal of Electronic and Computer Engineering, Vol. 6, No.1,2013.

[16] J. J. E. Slotine and W. Li, "Applied Nonlinear Control," Englewood Cliffs, NJ: Prentice–Hall, 1991.

[17] W. J. Wang and J. Y. Chen, "Passivity-based sliding mode position control for induction motor drives," In: IEEE Trans. On Energy Conversion, Vol. 20, No. 2, pp. 316-321, June 2005.

[18] M. Rashed, K. B. Goh, M. W. Dunnigan, P. F. A. MacConnell, A. F. Stronach and B. W. Williams, "Sensorless second-order sliding-mode speed control of a voltage-fed induction-motor drive using nonlinear state feedback," In: IEE Proc.-Electr. Power Appl., Vol. 152, No. 5, pp. 1127-1136, September 2005.

[19] A. Levant and L. Alelishvili, "Integral high-order sliding modes," In : IEEE Trans. Autom. Control, Vol. 52, No. 7, pp. 1278-1282, July 2007.

[20] S. Benelghali, M. E. H. Benbouzid, J. F. Charpentier, T. Ahmed-Ali, I. Munteanu, "Experimental validation of a marine current turbine simulator: Application to a PMSG-based system second-order sliding mode control," In: IEEE Trans. Ind. Elec., Vol. 58, No. 1, pp. 118-126, January 2011.

Zinelaabidine Boudjema was born in Algeria, in 1983. He received the PhD degree in electrical engineering from Djillali Liabes University, Sidi Bel-Abbes, Algeria, in February 2015. He is currently an associate professor at electrical engineering department at Hassiba Benbouali University. His research activities consist of robust control strategies, power electronics, electrical machine drives and renewable energies.

Rachid Taleb was born in Chlef, Algeria, in 1974. He received the PhD. degree in electrical engineering from the Djillali Liabes University, Sidi Bel-Abbes, Algeria, in 2011. He is currently an associate professor at the department of electrical engineering, Hassiba Benbouali University. His research interest includes intelligent control, heuristic optimization, control theory of converters and converters for renewable energy sources.

Adil yahdou was born in Chlef, Algeria, in 1983. He is a PhD student in Electrical Engineering Department at National Polytechnic School, Algies, Algeria. He received the M.S. degree in Electrical Engineering from Hassiba Benbouali University, Chlef, Algeria, in 2012. His research interest includes intelligent control, control theory of converters and converters for renewable energy sources.

Housseyn Kahal was born in Chlef, Algeria, in 1983. He is currently a PhD student in the Department of Electrical Engineering at Hassiba Benbouali University, Chlef, Algeria. He received the M.S. degree in Electrical Engineering from Mohamed Boudiaf University of Science and Technology, Oran, Algeria, in 2014. His research interest includes intelligent control strategies, electrical machine drives and renewable energies.